PHYSICAL REVIEW D **79,** 074027 (2009)

Tensor charges of light baryons in the infinite momentum frame

Cédric Lorcé*

Institut für Kernphysik, Johannes Gutenberg-Universität, D-55099 Mainz, Germany

(Received 10 December 2008; revised manuscript received 26 March 2009; published 30 April 2009)

We have used the chiral-quark soliton model formulated in the infinite momentum frame to investigate the octet, decuplet, and antidecuplet tensor charges up to the $5Q$ sector. Using flavor $SU(3)$ symmetry we have obtained for the proton $\delta u = 1.172$ and $\delta d = -0.315$ in fair agreement with previous model estimations. The $5Q$ contribution allowed us to estimate also the strange contribution to the proton tensor charge $\delta s = -0.011$. All those values have been obtained at the model scale $Q_0^2 = 0.36\ \text{GeV}^2$.

DOI: 10.1103/PhysRevD.79.074027 PACS numbers: 12.39.Fe

I. INTRODUCTION

Many nucleon properties can be characterized by parton distributions in hard processes. At the leading-twist level, there have been considerable efforts both theoretically and experimentally to determine the unpolarized $f_1(x)$ and longitudinally polarized (or helicity) $g_1(x)$ quark-spin distributions. In fact, a third structure function exists and is called the transversity distribution $h_1(x)$ [1]. The functions f_1, g_1, h_1 are, respectively, spin-average, chiral-even, and chiral-odd spin distributions. Only f_1 and g_1 contribute to deep-inelastic scattering when small quark-mass effects are ignored. Nevertheless, the function h_1 can be measured in certain physical processes such as polarized Drell-Yan processes [1] and other exclusive hard reactions [2–4]. Let us stress however that $h_1(x)$ does not represent the quark transverse-spin distribution. The transverse-spin operator does not commute with the free-particle Hamiltonian. In the light-cone formalism the transverse-spin operator is a bad operator and depends on the dynamics. This would explain why the interest in transversity distributions is rather recent. The interested reader can find a review of the subject in [5].

The present study uses the framework of the chiral-quark soliton model (χQSM), where a baryon is seen as three constituent quarks bound by a self-consistent mean classical pion field [6]. This model is fully relativistic and describes in a natural way the quark-antiquark sea. It has been recently formulated in the infinite momentum frame (IMF) [7,8], providing a new approach for extracting pre- and postdictions out of the model. Just like in the case of vector and axial charges, the IMF (or equivalently light-cone) formulation is particularly well suited to compute tensor charges. One can choose to work in a specific frame where the annoying part of the current, i.e. pair creation and annihilation part, does not contribute. Moreover, the concept of wave function is well defined in this frame, and one can more easily take relativistic effects into account.

The technique has already been used to study vector and axial charges of the nucleon and Θ^+ pentaquark width up to the $7Q$ component [8–10]. It has been shown that relativistic effects (i.e. quark angular momentum and additional quark-antiquark pairs) are essential to understand the nucleon structure. For example, they explain the reduction of the naive quark model value $5/3$ for the nucleon axial charge $g_A^{(3)}$ down to a value close to 1.257 observed in β decays.

In this paper, we present our results concerning octet, decuplet and antidecuplet tensor charges. We briefly explain the χQSM approach on the light cone and give an explicit definition of quantities needed for the computation in Sec. II. We proceed in Sec. III with a discussion on the Melosh rotation approach usually used in light-cone models compared to the χQSM one. Then, in Sec. IV, we discuss briefly tensor charges and Soffer's inequality. In Sec. V, we explain how matrix elements can be computed, and we express the physical quantities as linear combinations of a few scalar overlap integrals. Our final results can be found in Sec. VI, where they are compared with the experimental knowledge to date.

II. χQSM ON THE LIGHT CONE

In this section, we will not give all the details of the approach since this has already been done elsewhere [8–10]. We will just remind the philosophy and the important results needed for the present study.

The chiral-quark soliton model (χQSM) is a model proposed to mimic low-energy QCD. It emphasizes the role of constituent quarks of mass M and pseudoscalar mesons as the relevant degrees of freedom and is based on the following effective Lagrangian:

$$\mathcal{L}_{\chi\text{QSM}} = \bar{\psi}(p)(\not{p} - MU^{\gamma_5})\psi(p), \tag{1}$$

where U^{γ_5} is a (flavor) $SU(3)$ matrix. We used the $SU(2)$ hedgehog *Ansatz* for the soliton field trivially embedded in $SU(3)$

$$U^{\gamma_5} = \begin{pmatrix} U_0 & 0 \\ 0 & 1 \end{pmatrix}, \qquad U_0 = e^{in^a\tau^a P(r)\gamma_5}, \tag{2}$$

with τ^a the usual $SU(2)$ Pauli matrices and $n^a = r^a/r$ the unit vector pointing in the direction of $\mathbf{r}$. Note that the

*lorce@kph.uni-mainz.de

hedgehog *Ansatz* implies that a rotation in ordinary space (n^a) can be compensated by a rotation in isospin space (τ^a). The profile function $P(r)$ is determined by topological constraints and minimization of the energy of the system.

Within this model it has been shown [7,8] that one can write a general expression for $SU(3)$ baryon wave functions

$$|\Psi_B\rangle = \Bigg[\prod_{\text{color}=1}^{N_C}\int (d\mathbf{p})F(\mathbf{p})a^\dagger(\mathbf{p})\Bigg]\exp\bigg(\int (d\mathbf{p}) \times (d\mathbf{p}')a^\dagger(\mathbf{p})W(\mathbf{p},\mathbf{p}')b^\dagger(\mathbf{p}')\bigg)|\Omega_0\rangle. \tag{3}$$

This expression may look somewhat complicated at first view but it is in fact really transparent. The model describes baryons as N_C quarks populating a discrete level with wave function $F(\mathbf{p})$ accompanied by a whole sea of quark-antiquark pairs represented by the coherent exponential. The wave function of such a quark-antiquark pair is $W(\mathbf{p},\mathbf{p}')$. For a specific baryon, one has to rotate each quark by a $SU(3)$-matrix R and each antiquark by $R^\dagger$ and project the whole wave function on the quantum number of the specific baryon $\int dRB_k^*(R)$, where $B_k^*(R)$ represents the way the baryon is transformed by $SU(3)$. We intentionally omitted spin, isospin, flavor, and color indices to keep things simple. The full expression can be found in [8]. This wave function is our basic tool and is supposed to provide a lot of information about all light baryons.

A. Discrete-level wave function

On the light cone the discrete-level wave function $F(\mathbf{p})$ is given by

$$F(\mathbf{p}) = F_{\text{lev}}(\mathbf{p}) + F_{\text{sea}}(\mathbf{p}), \tag{4}$$

with

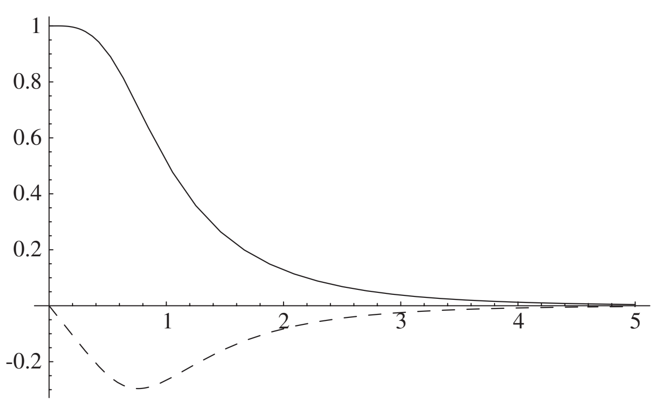

FIG. 1. Upper s-wave component $h(r)$ (solid) and lower p-wave component $j(r)$ (dashed) of the bound-state quark level in light baryons. Each of the three discrete-level quarks has energy $E_{\text{lev}} = 200$ MeV. Horizontal axis has units of $1/M = 0.57$ fm.

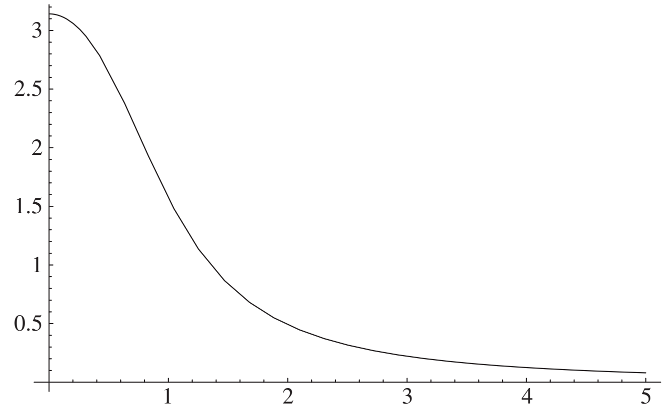

FIG. 2. Profile of the self-consistent chiral field $P(r)$ in light baryons. The horizontal axis unit is $r_0 = 0.8/M = 0.46$ fm.

$$F^{j\sigma}_{\text{lev}}(z,\mathbf{p}_\perp) = \sqrt{\frac{\mathcal{M}}{2\pi}}\bigg[\epsilon^{j\sigma}h(p) + (p_z\mathbb{1} + i\mathbf{p}_\perp \times \boldsymbol{\tau}_\perp)^\sigma_{\sigma'}\epsilon^{j\sigma'}\frac{j(p)}{|\mathbf{p}|}\bigg]_{p_z=z\mathcal{M}-E_{\text{lev}}}, \tag{5}$$

$$F^{j\sigma}_{\text{sea}}(z,\mathbf{p}_\perp) = -\sqrt{\frac{\mathcal{M}}{2\pi}}\int dz'\frac{d^2\mathbf{p}'_\perp}{(2\pi)^2}W^{j\sigma}_{j'\sigma'}(z,\mathbf{p}_\perp;z',\mathbf{p}'_\perp)\epsilon^{j'\sigma''} \times \bigg[(\tau_3)^{\sigma'}_{\sigma''}h(p') - (\mathbf{p}'\cdot\tau)^{\sigma'}_{\sigma''}\frac{j(p')}{|\mathbf{p}'|}\bigg]_{p_z=z\mathcal{M}-E_{\text{lev}}}, \tag{6}$$

where j and σ are isospin and spin indices, respectively, z is the fraction of baryon longitudinal momentum carried by the quark, $\mathbf{p}_\perp$ is its transverse momentum, and $\mathcal{M}$ is the classical soliton mass. In this study, we neglect the distortion of the discrete level due to the sea F_{sea}, which is quite time consuming and can reasonably be expected to be small compared to the undistorted discrete-level contribution F_{lev}. It is however difficult to estimate exactly its impact without an explicit computation.

The functions $h(p)$ and $j(p)$ are Fourier transforms of the upper ($L = 0$) $h(r)$ and lower ($L = 1$) $j(r)$ components of the spinor solution (see Fig. 1) of the static Dirac equation in the mean field with eigenenergy[1] E_{lev}

$$\begin{gathered}\psi_{\text{lev}}(\mathbf{x}) = \begin{pmatrix}\epsilon^{ji}h(r)\\ -i\epsilon^{jk}(\mathbf{n}\cdot\boldsymbol{\sigma})^i_k j(r)\end{pmatrix},\\ h' + hM\sin P - j(M\cos P + E_{\text{lev}}) = 0,\\ j' + 2j/r - jM\sin P - h(M\cos P - E_{\text{lev}}) = 0,\end{gathered} \tag{7}$$

where $P(r)$, the profile function of the soliton, is fairly approximated by [6,11] (see Fig. 2)

[1]This eigenenergy turned out to be $E_{\text{lev}} \approx 200$ MeV when solving the system of equations self-consistently for constituent quark mass $M = 345$ MeV.

$$P(r) = 2\arctan\left(\frac{r_0^2}{r^2}\right), \qquad r_0 \approx \frac{0.8}{M}. \tag{8}$$

B. Pair wave function

The quark-antiquark pair wave function $W(\mathbf{p}, \mathbf{p}')$ can be written in terms of the Fourier transform of the chiral field with chiral circle condition $\Pi^2 + \Sigma^2 = 1$, $U_0 = \Sigma + i\Pi\gamma_5$. The chiral field is then given by

$$\Pi = \mathbf{n}\cdot\boldsymbol{\tau}\sin P(r), \qquad \Sigma(r) = \cos P(r)$$

and its Fourier transform by

$$\Pi(\mathbf{q})^j_{j'} = \int d^3\mathbf{x} e^{-i\mathbf{q}\cdot\mathbf{x}}(\mathbf{n}\cdot\tau)^j_{j'}\sin P(r),$$
$$\Sigma(\mathbf{q})^j_{j'} = \int d^3\mathbf{x} e^{-i\mathbf{q}\cdot\mathbf{x}}(\cos P(r) - 1)\delta^j_{j'},$$

where j and j' are the isospin indices of the quark and antiquark, respectively. The pair wave function is obtained by considering the expansion of the quark propagator [7] in the mean field in terms of the chiral interaction $V = U_0 - 1$. After the boost to the IMF, the pair wave function appears as a function of the fractions of the baryon longitudinal momentum carried by the quark z and antiquark z' of the pair and their transverse momenta $\mathbf{p}_\perp$, $\mathbf{p}'_\perp$

$$W^{j\sigma}_{j'\sigma'}(y, \mathbf{q}, \mathcal{Q}_\perp) = \frac{M\mathcal{M}}{2\pi}\frac{\Sigma^j_{j'}(\mathbf{q})[M(2y-1)\tau_3 + \mathcal{Q}_\perp\cdot\boldsymbol{\tau}_\perp]^\sigma_{\sigma'} + i\Pi^j_{j'}(\mathbf{q})[-M\mathbb{1} + i\mathcal{Q}_\perp\times\boldsymbol{\tau}_\perp]^\sigma_{\sigma'}}{\mathcal{Q}_\perp^2 + M^2 + y(1-y)\mathbf{q}^2}, \tag{9}$$

with

$$y = \frac{z'}{z+z'}, \qquad \mathcal{Q}_\perp = \frac{z\mathbf{p}'_\perp - z'\mathbf{p}_\perp}{z+z'},$$

and where $\mathbf{q} = ((\mathbf{p}+\mathbf{p}')_\perp, (z+z')\mathcal{M})$ is the three-momentum of the pair as a whole transferred from the background fields $\Sigma(\mathbf{q})$ and $\Pi(\mathbf{q})$. As earlier j and j' are isospin, and σ and σ' are spin indices with the prime for the antiquark.

C. Rotational wave function

To obtain the wave function of a specific baryon with given spin projection k, one has to rotate the soliton in ordinary and flavor spaces and then project on quantum numbers of this specific baryon. For example, one has to compute the following integral to obtain the neutron rotational wave function in the $3Q$ sector

$$T(n^0)^{f_1f_2f_3}_{k,j_1j_2j_3} = \int dR\, n_k(R)^* R^{f_1}_{j_1}R^{f_2}_{j_2}R^{f_3}_{j_3}, \tag{10}$$

where R is a $SU(3)$ matrix, and $n_k(R)^* = \frac{\sqrt{8}}{24}\epsilon_{kl}R^{\dagger l}_2 R^3_3$ represents the way that the neutron is transformed under $SU(3)$ rotations. This integral means that the neutron state $n_k(R)^*$ is projected onto the $3Q$ sector $R^{f_1}_{j_1}R^{f_2}_{j_2}R^{f_3}_{j_3}$ by means of the integration over all $SU(3)$ matrices $\int dR$. By contracting this rotational wave function $T(n^0)^{f_1f_2f_3}_{k,j_1j_2j_3}$ with the nonrelativistic $3Q$ wave function[2] $\epsilon^{j_1\sigma_1}\epsilon^{j_2\sigma_2}\epsilon^{j_3\sigma_3}\times h(p_1)h(p_2)h(p_3)$ one finally obtains the nonrelativistic neutron wave function

$$|n^0\rangle_k^{f_1f_2f_3,\sigma_1\sigma_2\sigma_3} = \frac{\sqrt{8}}{24}\epsilon^{f_1f_2}\epsilon^{\sigma_1\sigma_2}\delta^{f_3}_2\delta^{\sigma_3}_k h(p_1)h(p_2)h(p_3)$$
$$+ \text{cyclic permutations of } 1, 2, 3. \tag{11}$$

This expression means[3] that there is a ud pair in spin-isospin zero combination $\epsilon^{f_1f_2}\epsilon^{\sigma_1\sigma_2}$ and that the third quark is a down quark $\delta^{f_3}_2$ carrying the whole spin of the neutron $\delta^{\sigma_3}_k$. This is in fact exactly the $SU(6)$ spin-flavor wave function for the neutron.

In the $5Q$ sector the neutron wave function in the momentum space is given by

$$\begin{aligned}
&(|n\rangle_k)^{f_1f_2f_3f_4,\sigma_1\sigma_2\sigma_3\sigma_4}_{f_5,\sigma_5}(\mathbf{p}_1\ldots\mathbf{p}_5)\\
&= \frac{\sqrt{8}}{360}F^{j_1\sigma_1}(\mathbf{p}_1)F^{j_2\sigma_2}(\mathbf{p}_2)F^{j_3\sigma_3}(\mathbf{p}_3)W^{j_4\sigma_4}_{j_5\sigma_5}(\mathbf{p}_4,\mathbf{p}_5)\\
&\quad\times\epsilon_{k'k}\{\epsilon^{f_1f_2}\epsilon_{j_1j_2}[\delta^{f_3}_2\delta^{f_4}_{f_5}(4\delta^{j_5}_{j_4}\delta^{k'}_{j_3} - \delta^{j_5}_{j_3}\delta^{k'}_{j_4})\\
&\quad+\delta^{f_4}_2\delta^{f_3}_{f_5}(4\delta^{j_5}_{j_3}\delta^{k'}_{j_4} - \delta^{j_5}_{j_4}\delta^{k'}_{j_3})]\\
&\quad+\epsilon^{f_1f_4}\epsilon_{j_1j_4}[\delta^{f_2}_2\delta^{f_3}_{f_5}(4\delta^{j_5}_{j_3}\delta^{k'}_{j_2} - \delta^{j_5}_{j_2}\delta^{k'}_{j_3})\\
&\quad+\delta^{f_3}_2\delta^{f_2}_{f_5}(4\delta^{j_5}_{j_2}\delta^{k'}_{j_3} - \delta^{j_5}_{j_3}\delta^{k'}_{j_2})]\}\\
&\quad+\text{permutations of } 1, 2, 3.
\end{aligned} \tag{12}$$

The color degrees of freedom are not explicitly written but the three discrete-level quarks (1,2,3) are still antisymmetric in color, while the quark-antiquark pair (4,5) forms a color singlet. Let us concentrate on the flavor part of this wave function. One can notice that it allows hidden flavors to access to the discrete level. The flavor structure of the neutron at the $5Q$ level is

$$|n\rangle = A|udd(u\bar{u})\rangle + B|udd(d\bar{d})\rangle + C|udd(s\bar{s})\rangle$$
$$+ D|uud(d\bar{u})\rangle + E|uds(d\bar{s})\rangle, \tag{13}$$

[2]The nonrelativistic limit here means that we neglect the lower component j of the Dirac field.

[3]One has $f = u, d, s$ and $\sigma = \uparrow, \downarrow$.

where the three first flavors belong to the discrete-level sector and the last two to the quark-antiquark pair. All rotational wave functions up to the $7Q$ sector can be found in the Appendix of [10].

III. COMPARISON WITH LIGHT-CONE CONSTITUENT QUARK MODEL

In this section, we would like to emphasize the differences of the present approach with the so-called light-cone constituent quark model (LCCQM) [12].

A. Standard light-cone approach

On the light cone, a baryon state $|\Psi_B\rangle$ can be regarded as the superposition of Fock states $|\mu_n\rangle$ [13]

$$|\Psi_B\rangle = \sum_n \int d[\mu_n]\psi_{n/B}|\mu_n\rangle, \tag{14}$$

where $\psi_{n/B}$, called wave function, is the projection of $|\Psi_B\rangle$ on the Fock state $|\mu_n\rangle$. The complete basis of Fock states is constructed by applying products of free-field creation operators to the vacuum state $|0\rangle$. These states are eigenstates of total light-cone three-momentum $(P^+, \mathbf{P}_\perp)$ with eigenvalues

$$\mathbf{P}_\perp = \sum_{i\in n}\mathbf{k}_{i\perp}, \qquad P^+ = \sum_{i\in n} k_i^+, \tag{15}$$

where $(k_i^+, \mathbf{k}_{i\perp})$ are the light-cone three-momenta of the particles in the given Fock state $|\mu_n\rangle$. Let us restrict ourselves to massive quanta only $m_i \neq 0$, so that we have $k_i^+ > 0$. Note also that all individual particles in a Fock state are on shell $k_i^2 = m_i^2$, i.e. $k_i^- = (m_i^2 + \mathbf{k}_{i\perp}^2)/k_i^+$. On the contrary, the Fock state itself is in general not on shell since the free-invariant mass squared

$$\mathcal{M}_0^2 = \tilde{P}^2, \qquad \tilde{P}^\mu \equiv \sum_{i\in n} k_i^\mu \tag{16}$$

is different from the bound-state mass squared $\mathcal{M}^2$. Because of interactions, the bound-state light-cone energy P^- is not simply the sum of the light-cone energies of constituents $\tilde{P}^- = \sum_{i\in n} k_i^-$.

On the light cone, since boosts are kinematical, one can easily separate the internal motion from the center-of-mass motion and therefore introduce relative variables. One can define boost-invariant longitudinal momentum fractions $z_i = k_i^+/P^+$ and relative transverse momenta $\mathbf{p}_{i\perp} = \mathbf{k}_{i\perp} - z_i\mathbf{P}_\perp$, which are constrained by

$$\sum_{i\in n} z_i = 1, \qquad \sum_{i\in n}\mathbf{p}_{i\perp} = \mathbf{0}. \tag{17}$$

The free-invariant mass squared does not depend on the light-cone three-momentum of the bound state, and can thus be expressed in terms of constituent masses and relative variables only

$$\mathcal{M}_0^2 = \sum_{i\in n}\frac{m_i^2 + \mathbf{p}_{i\perp}^2}{z_i}. \tag{18}$$

The baryon state can be written as

$$|\Psi_B\rangle = \sum_n \sum_{\lambda_i\in n}\int [dz_i][d^2p_{i\perp}]\psi_{n/B}(z_i, \mathbf{p}_{i\perp}, \lambda_i) \times |n, z_iP^+, \mathbf{p}_{i\perp} + z_iP^+, \lambda_i\rangle, \tag{19}$$

where λ_i are the light-cone helicities of the constituents, and with

$$[dz_i] = \delta\Big(1 - \sum_{i\in n} z_i\Big)\prod_{i\in n} dz_i, \qquad [d^2p_{i\perp}] = (2\pi)^2\delta^{(2)}\Big(\sum_{i\in n}\mathbf{p}_{i\perp}\Big)\prod_{i\in n}\frac{d^2p_{i\perp}}{(2\pi)^2}. \tag{20}$$

B. Light-cone constituent quark model

The LCCQM assumes that a baryon bound state can be represented by an effective $3Q$ wave function. In order to obtain a hadron state of definite spin, it is convenient to define relative longitudinal components as [14]

$$p_{i3} = \frac{1}{2}\Big(\mathcal{M}_0 z_i - \frac{m_i^2 + \mathbf{p}_{i\perp}^2}{\mathcal{M}_0 z_i}\Big), \tag{21}$$

such that the relative momenta $\mathbf{p}_i = (\mathbf{p}_{i\perp}, p_{i3})$ and the spin satisfy vector commutation relations. In this constituent rest frame $\sum_{i\in n}\mathbf{p}_i = \mathbf{0}$ one can identify the free-invariant mass with the sum of constituent instant-form energies

$$\mathcal{M}_0 = \tilde{P}^0 = \sum_{i\in n}\sqrt{\mathbf{p}_i^2 + m_i^2}. \tag{22}$$

Moreover, the total spin operator $\mathbf{J}$ can be expressed as a sum of orbital and spin contributions

$$\mathbf{J} = \sum_i(\mathbf{y}_i \times \mathbf{p}_i + \mathbf{j}_i), \tag{23}$$

where $\mathbf{y}_i$ are coordinate operators of quarks, and the operators $\mathbf{j}_i$ are related to the quark spin $\mathbf{s}_i$ by a Melosh rotation [15]

$$\mathbf{j}_i = \mathcal{R}_M(z_i, \mathbf{p}_{i\perp}, m_i, \mathcal{M}_0)\mathbf{s_i}, \tag{24}$$

whose $SU(2)$ matrix representation is

$$D^{1/2}(\mathcal{R}_M) = \frac{(m_i + z_i\mathcal{M}_0)\mathbb{1} + i\mathbf{n}\cdot(\boldsymbol{\sigma}\times\mathbf{p}_{i\perp})}{\sqrt{(m_i + z_i\mathcal{M}_0)^2 + \mathbf{p}_{i\perp}^2}}, \tag{25}$$

where $\mathbf{n} = (0, 0, 1)$ and $\boldsymbol{\sigma}$ are the Pauli matrices. For more details concerning Melosh rotation, see the Appendix.

Expressed in terms of the relative momenta $\mathbf{p}_i$ and the eigenvalues of $\mathbf{j}_3$, the wave function has the same structure as the NQM one. Furthermore, assuming that all quarks are in a s-state, the NQM wave function has only one spin-isospin structure. In LCCQM, one therefore tries to describe baryon properties in terms of only one scalar function, corresponding to the radial part of the NQM wave function.

C. Differences with our approach

In χQSM, we rely on a mean field approach. Three constituent quarks are not sufficient to describe baryons, and so an infinite tower of quark-antiquark pairs is involved. Light-cone wave functions coincide with instant-form wave function in the IMF [16]. Usually, such a boost to IMF is not achievable because of interactions. Nevertheless, thanks to the mean field approach and the fact that χQSM is a fully relativistic model, the light-cone wave functions have been derived.

Looking at the undistorted discrete-level wave function (5), one notices similarities with the Melosh rotation (25) involved in LCCQM. Note however that our undistorted discrete-level wave function involves *two* scalar functions, in contrast to the Melosh rotation, which is just multiplied by *one* scalar function in LCCQM. Remember that in the latter, one makes the dynamical assumption that all quarks are in a s-state, so that no arbitrariness is left in the spin-flavor structure of the wave function. In this case, the orbital angular momentum has purely kinematical origin as it comes from the Melosh rotation only. However, such an assumption can only be valid in a nonrelativistic system. In χQSM, constituent quarks are treated relativistically and can therefore be in a p state. Orbital angular momentum then also receives a dynamical contribution [17]. The spin-flavor structure of the wave function is uniquely determined by the projection of the rotating soliton onto quantum numbers of the baryon. Clearly, χQSM is a more sophisticated and realistic model.

Note however that in the nonrelativistic limit, the two models coincide. Indeed, in this limit quark momenta are small compared to the quark mass, and one can neglect the p-state contribution. Quarks are therefore collinear and helicity structure is no more affected by the transverse motion of quarks.

IV. TENSOR CHARGES

The tensor charges of a baryon are defined as forward matrix elements of the tensor current

$$\langle B(p)|\bar{\psi} i\sigma^{\mu\nu}\gamma_5\lambda^a\psi|B(p)\rangle = g_T^{(a)}\bar{u}(p)i\sigma^{\mu\nu}\gamma_5 u(p), \quad (26)$$

where $a = 0, 3, 8$ and λ^3, λ^8 are Gell-Mann matrices, λ^0 is just in this context the 3×3 unit matrix. These tensor charges are related to the first moment of the transversely polarized quark distributions

$$g_T^{(3)} = \delta u - \delta d, \qquad g_T^{(8)} = \frac{1}{\sqrt{3}}(\delta u + \delta d - 2\delta s), \quad g_T^{(0)} = \delta u + \delta d + \delta s, \quad (27)$$

where $\delta q \equiv \int_0^1 dz[q_\uparrow(z) - q_\downarrow(z) - \bar{q}_\uparrow(z) + \bar{q}_\downarrow(z)]$ with $q = u, d, s$ and using the transversity basis [18] for a nucleon travelling along the z axis with its polarization along the x axis

$$|\uparrow\rangle = \frac{1}{\sqrt{2}}(|+\rangle + |-\rangle), \qquad |\downarrow\rangle = \frac{1}{\sqrt{2}}(|+\rangle - |-\rangle) \quad (28)$$

written in terms of the usual helicity eigenstates $|\pm\rangle$. We split the tensor charges into discrete-level quark, sea quark, and antiquark contributions

$$\delta q = \delta q_{\rm lev} + \delta q_{\rm sea}, \qquad \delta q_{\rm sea} = \delta q_{\rm s} - \delta\bar{q}, \quad (29)$$

where index s refers to the quarks in the sea pairs. The tensor charges just count the total number of quarks with transverse polarization aligned *minus* total number of quarks with transverse polarization anti-aligned with baryon polarization.

A. Tensor charges vs axial charges

Based on naive rotational invariance considerations, one might think that tensor and axial charges are actually equal $\delta q = \Delta q$. In deep-inelastic scattering, quarks in the nucleon appear to be free, but rotational invariance has become nontrivial since high-energy processes select a special direction. In the IMF these rotations involve interactions [19]. The difference between axial and tensor charges has in fact a *dynamical origin*. Only in nonrelativistic quark models the transverse-spin operator commutes with a free-quark Hamiltonian, and so transversely polarized quarks are in transverse-spin eigenstates. Then rotational invariance implies $\delta q = \Delta q$. This can also be seen from the tensor current $\bar{\psi} i\sigma^{0i}\gamma_5\psi$, which differs from the axial-vector current $\bar{\psi}\gamma^i\gamma_5\psi$ by a factor γ^0. This factor is reduced to 1 in the nonrelativistic limit.

The second point we would like to emphasize is that the tensor quark bilinear is odd under charge conjugation. This means that we have to consider the contribution of quarks $\delta q_{\rm lev} + \delta q_{\rm s}$ *minus* the contribution of antiquarks $\delta\bar{q}$, just like in the case of vector charges. On the contrary, the axial quark bilinear is even under charge conjugation. This means that we have to consider the contribution of quarks $\Delta q_{\rm lev} + \Delta q_{\rm s}$ *plus* the contribution of antiquarks $\Delta\bar{q}$.

B. Discrete-level, valence and constituent quarks

In this subsection, we would like to explain clearly the distinction between valence quarks and discrete-level quarks, in order to clarify further statements.

(i) Valence quarks refer to objects that give the quantum numbers of the baryon, e.g. from the proton sum rules $\int dz[u(z) - \bar{u}(z)] = 2$ and $\int dz[d(z) - \bar{d}(z)] = 1$ one says that there are two up valence quarks and one down valence quark.

(ii) Discrete-level quarks are those quarks that fill in the discrete level of the spectrum in our approach.

How are these related to the notion of constituent quarks?

The main problem in the literature is that the concept of constituent quarks is not clearly defined. All the pictures do however agree on the fact that constituent quarks U, D, S are some kind of nonperturbative objects, which consist of QCD (or current) quarks u, d, s dressed by strong interaction and having an effective mass of about 350 MeV. We will distinguish three different pictures:

(1) *Constituent quarks only*—In this picture, one believes that the effects of all the gluons and quark-antiquark pairs are included effectively in the constituent quarks. This is the old picture of the nonrelativistic constituent quark model or naive quark model [20]. Baryons are therefore made of three constituent quarks only. For example, the proton is just a UUD bound state. Since no explicit antiquarks are present, these constituent quarks can be identified with valence quarks.

(2) *Constituent quarks + perturbative sea*—In this picture, one believes that the effects of all the gluons and quark-antiquark pairs cannot be included effectively in the constituent quarks only. Explicit quark-antiquark pairs have to be added to form baryons. Baryons are therefore made of three constituent quarks *plus* a sea of gluons and quark-antiquark pairs. This sea is described by the perturbative gluons splitting process into pairs of quark and antiquark with the same flavor and distribution $g \to q_f \bar{q}_f$, while constituent quarks are unchanged. For example, the proton is just a UUD *plus* an indefinite number of $q_f \bar{q}_f$ bound state. Since the quarks and antiquarks of this sea have the same distribution $q_f(z) - \bar{q}_f(z) = 0$, one can once more identify constituent quarks with valence quarks.

(3) *Constituent quarks + nonperturbative sea*—In this picture, contrarily to the previous one, one considers that besides gluon splitting processes constituent quarks can fluctuate, see e.g. [21]. Roughly speaking, this means that a constituent quark U can emit a $u\bar{d}$ pair and become a D constituent quark. This process is nonperturbative since it corresponds to the emission of quarks and antiquarks by a nonperturbative object. Baryons are still made of three constituent quarks *plus* a sea of gluons and quark-antiquark pairs, but flavors are allowed to have different assignments. For example, the proton is now a complicated mixture of UUD, $UUD + q_f\bar{q}_f$, $UDD + u\bar{d}$, $USD + u\bar{s}$, and so on. Since it is very unlikely that U and u have the same distribution, one cannot identify constituent quarks with valence quarks anymore. The proton sum rules are however still satisfied. In this picture, it becomes clear that valence quarks are indeed fictitious objects convenient for the baryon classification, just like how Gell-Mann considered them originally, and cannot be identified with any physical object.

As one can see, out of the three pictures, the third is the most general. This nonperturbative picture has been described with many variations. For example, the fluctuation $UUD \to UDD + u\bar{d}$ is seen in a meson-baryon fluctation approach as $p^+ \to n^0 + \pi^+$. In the chiral-quark model, one considers that constituent quarks emit perturbatively chiral mesons. In our approach, the discrete-level quarks are the massive effective quarks arising from spontaneous chiral symmetry breaking and can therefore be identified with the constituent quarks. All the flavor configurations are obtained by means of chiral rotations of the mean field bounding the discrete-level quarks.

We are now ready to discuss the link with tensor charges. Usually in the literature (see e.g. [2]), one claims that only valence quarks contribute to tensor charges. As corollary, there cannot be any contribution from strangeness to the proton tensor charges. These claims are actually only valid in the first two pictures. In the more general third picture, it is simply wrong, and so strangeness contribution to the proton tensor charge is actually possible. Nevertheless, since one expects the $3Q$ component of the proton wave function to be dominant, this strangeness contribution arising from higher Fock sectors should be small.

C. Soffer's inequality

Based on general grounds, very little is known concerning tensor charges. That is why one usually has to rely on model predictions. However, Soffer [22] has proposed an inequality among the nucleon twist-2 quark distributions f_1, g_1, h_1

$$f_1 + g_1 \geq 2|h_1|. \tag{30}$$

Vector, axial and tensor charges just correspond to the first moment of the leading-twist quark distributions f_1, g_1 and h_1, respectively.

In contrast to the well-known inequalities and positivity constraints among distribution functions such as $f_1 \geq |g_1|$, which are general properties of lepton-hadron scattering, derived without reference to quarks, color or QCD, this Soffer inequality needs a parton model to QCD to be derived [23]. Unfortunately, it turns out that it does not constrain much the nucleon tensor charge. However, this inequality still has to be satisfied by models that try to estimate quark distributions.

D. Matrix elements on the light cone

The tensor charge can be obtained in IMF by means of the *plus* component of the tensor operator

$$\delta q \equiv \frac{1}{2P^+}\left\langle P, \frac{1}{2} \,\middle|\, \bar{\psi}_{\rm LC}\gamma^+\gamma^R\psi_{\rm LC} \,\middle|\, P, -\frac{1}{2}\right\rangle, \tag{31}$$

where $\gamma^R = (\gamma^1 + i\gamma^2)/2$. If one uses the Drell frame $q^+ = 0$ [13,24], where q is the total momentum transfer then the tensor current cannot create nor annihilate any quark-antiquark pair. This is a big advantage of the light-

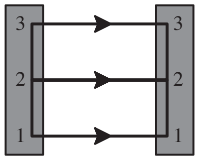

FIG. 3. Schematic representation of the $3Q$ normalization. Each quark line stands for the color, flavor, and spin contractions $\delta^{\alpha_i}_{\alpha'_i}\delta^{f_i}_{f'_i}\delta^{\sigma_i}_{\sigma'_i}\int dz'_i d^2\mathbf{p}'_{i\perp}\delta(z_i - z'_i)\delta^{(2)}(\mathbf{p}_{i\perp} - \mathbf{p}'_{i\perp})$. The large dark rectangles stand for the three initial (left) and final (right) discrete-level quarks antisymmetrized in color $\epsilon_{\alpha_1\alpha_2\alpha_3}$.

cone formulation since one needs to compute diagonal transitions only, i.e. $3Q$ into $3Q$, $5Q$ into $5Q, \ldots$ and not $3Q$ into $5Q$, for example.

In the $3Q$ sector, since all (discrete-level) quarks are on the same footing, all the possible contractions of creation-annihilation operators are equivalent. One can use a diagram to represent these contractions. The contractions without any current operator acting on a quark line correspond to the normalization of the state. We choose the simplest one where all quarks with the same label are connected, see Fig. 3.

In the $5Q$ sector, all contractions are equivalent to either the so-called "direct" diagram or the "exchange" diagram, see Fig. 4. In the direct diagram, all quarks with the same label are connected, while in the exchange one, a discrete-level quark is exchanged with the quark of the sea pair. It has appeared in a previous work [9] that exchange diagrams do not contribute much and can thus be neglected (there is no disconnected quark loop). So we use only the direct contributions throughout this paper. Moreover, one can reasonably consider that the $7Q$ contribution (and therefore higher contributions) will not be very significant [10].

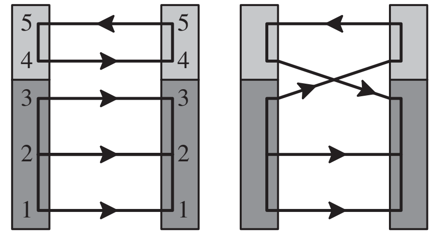

FIG. 4. Schematic representation of the $5Q$ direct (left) and exchange (right) contributions to the normalization. The quark-antiquark pairs are represented by small light rectangles and are in color singlet $\delta^{\alpha_4}_{\alpha_5}$.

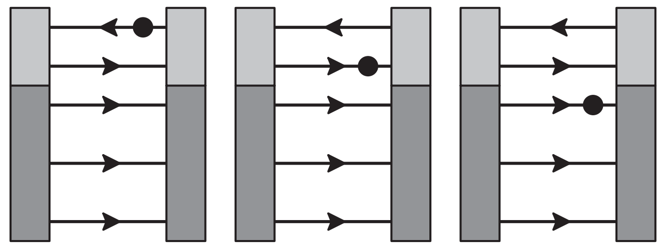

FIG. 5. Schematic representation of the three types of $5Q$ contributions to the charges: antiquark (left), sea quark (center), and discrete-level quark (right) contributions.

The operator acts on each quark line. In the present approach it is then easy to compute separately contributions coming from the discrete-level quarks, the sea quarks or antiquarks, see Fig. 5. These diagrams represent some contraction of color, spin, isospin, and flavor indices. For example, the sum of the three diagrams in the $5Q$ sector with the vector current $\bar{\psi}\gamma^+\psi$ acting on the quark lines represents the following expression:

$$V^{(5)}(1\to 2) = \frac{108}{2}\delta^k_l T(1)^{f_1f_2f_3f_4,j_5}_{j_1j_2j_3j_4,f_5,k} T(2)^{l_1l_2l_3l_4,g_5,l}_{f_1f_2g_3g_4,l_5}\int (dp_{1-5}) F^{j_1\sigma_1}(\mathbf{p}_1)F^{j_2\sigma_2}(\mathbf{p}_2)F^{j_3\sigma_3}(\mathbf{p}_3)W^{j_4\sigma_4}_{j_5\sigma_5}(\mathbf{p}_4,\mathbf{p}_5)F^\dagger_{l_1\sigma_1}(\mathbf{p}_1)F^\dagger_{l_2\sigma_2}(\mathbf{p}_2)$$
$$\times F^\dagger_{l_3\tau_3}(\mathbf{p}_3)W^{l_5\tau_5}_{cl_4\tau_4}(\mathbf{p}_4,\mathbf{p}_5)[-\delta^{g_3}_{f_3}\delta^{g_4}_{f_4}\boldsymbol{J}^{f_5}_{g_5}\delta^{\tau_3}_{\sigma_3}\delta^{\tau_4}_{\sigma_4}\boldsymbol{\delta}^{\sigma_5}_{\tau_5} + \delta^{g_3}_{f_3}\boldsymbol{J}^{g_4}_{f_4}\delta^{f_5}_{g_5}\delta^{\tau_3}_{\sigma_3}\boldsymbol{\delta}^{\tau_4}_{\sigma_4}\delta^{\sigma_5}_{\tau_5} + 3\boldsymbol{J}^{g_3}_{f_3}\delta^{g_4}_{f_4}\delta^{f_5}_{g_5}\boldsymbol{\delta}^{\tau_3}_{\sigma_3}\delta^{\tau_4}_{\sigma_4}\delta^{\sigma_5}_{\tau_5}], \quad (32)$$

where J^f_g is the flavor content of the current.

V. SCALAR OVERLAP INTEGRALS

The contractions in the previous section are easily performed by MATHEMATICA over all flavor (f, g), isospin (j, l) and spin (σ, τ) indices. One is then left with scalar integrals over longitudinal z and transverse $\mathbf{p}_\perp$ momenta of the quarks. The integrals over relative transverse momenta in the quark-antiquark pair are generally UV divergent. We have chosen to use the Pauli-Villars regularization with mass $M_{\rm PV} = 556.8$ MeV (this value being chosen from the requirement that the pion decay constant $F_\pi = 93$ MeV is reproduced from $M = 345$ MeV).

For convenience, we introduce the probability distribution $\Phi^I(z, \mathbf{q}_\perp)$ that three discrete-level quarks leave the longitudinal fraction $z = q_z/\mathcal{M}$ and the transverse momentum $\mathbf{q}_\perp$ to the quark-antiquark pair(s) as seen by a vector $(I = V)$ or a tensor $(I = T)$ probe

$$\Phi^I(z, \mathbf{q}_\perp) = \int dz_{1,2,3}\frac{d^2\mathbf{p}_{1,2,3\perp}}{(2\pi)^6}\delta(z + z_1 + z_2 + z_3 - 1)$$
$$\times (2\pi)^2\delta^{(2)}(\mathbf{q}_\perp + \mathbf{p}_{1\perp} + \mathbf{p}_{2\perp} + \mathbf{p}_{3\perp})$$
$$\times D^I(p_1, p_2, p_3). \quad (33)$$

The function $D^I(p_1, p_2, p_3)$ is given in terms of the upper and lower discrete-level wave functions $h(p)$ and $j(p)$ as follows:

$$\begin{aligned} D^V(p_1, p_2, p_3) = {} & h^2(p_1)h^2(p_2)h^2(p_3) + 6h^2(p_1)h^2(p_2)\left[h(p_3)\frac{p_{3z}}{|\mathbf{p}_3|}j(p_3)\right] + 3h^2(p_1)h^2(p_2)j^2(p_3) \\ & + 12h^2(p_1)\left[h(p_2)\frac{p_{2z}}{|\mathbf{p}_2|}j(p_2)\right]\left[h(p_3)\frac{p_{3z}}{|\mathbf{p}_3|}j(p_3)\right] + 12h^2(p_1)\left[h(p_2)\frac{p_{2z}}{|\mathbf{p}_2|}j(p_2)\right]j^2(p_3) \\ & + 8\left[h(p_1)\frac{p_{1z}}{|\mathbf{p}_1|}j(p_1)\right]\left[h(p_2)\frac{p_{2z}}{|\mathbf{p}_2|}j(p_2)\right]\left[h(p_3)\frac{p_{3z}}{|\mathbf{p}_3|}j(p_3)\right] + 3h^2(p_1)j^2(p_2)j^2(p_3) \\ & + 12\left[h(p_1)\frac{p_{1z}}{|\mathbf{p}_1|}j(p_1)\right]\left[h(p_2)\frac{p_{2z}}{|\mathbf{p}_2|}j(p_2)\right]j^2(p_3) + 6\left[h(p_1)\frac{p_{1z}}{|\mathbf{p}_1|}j(p_1)\right]j^2(p_2)j^2(p_3) \\ & + j^2(p_1)j^2(p_2)j^2(p_3), \end{aligned} \tag{34}$$

$$\begin{aligned} D^T(p_1, p_2, p_3) = {} & h^2(p_1)h^2(p_2)h^2(p_3) + 6h^2(p_1)h^2(p_2)\left[h(p_3)\frac{p_{3z}}{|\mathbf{p}_3|}j(p_3)\right] + h^2(p_1)h^2(p_2)\frac{p_{3z}^2 + 2p_3^2}{p_3^2}j^2(p_3) \\ & + 12h^2(p_1)\left[h(p_2)\frac{p_{2z}}{|\mathbf{p}_2|}j(p_2)\right]\left[h(p_3)\frac{p_{3z}}{|\mathbf{p}_3|}j(p_3)\right] + 4h^2(p_1)\left[h(p_2)\frac{p_{2z}}{|\mathbf{p}_2|}j(p_2)\right]\frac{p_{3z}^2 + 2p_3^2}{p_3^2}j^2(p_3) \\ & + 8\left[h(p_1)\frac{p_{1z}}{|\mathbf{p}_1|}j(p_1)\right]\left[h(p_2)\frac{p_{2z}}{|\mathbf{p}_2|}j(p_2)\right]\left[h(p_3)\frac{p_{3z}}{|\mathbf{p}_3|}j(p_3)\right] + h^2(p_1)j^2(p_2)\frac{2p_{3z}^2 + rp_3^2}{p_3^2}j^2(p_3) \\ & + 4\left[h(p_1)\frac{p_{1z}}{|\mathbf{p}_1|}j(p_1)\right]\left[h(p_2)\frac{p_{2z}}{|\mathbf{p}_2|}j(p_2)\right]\frac{p_{3z}^2 + 2p_3^2}{p_3^2}j^2(p_3) + 2\left[h(p_1)\frac{p_{1z}}{|\mathbf{p}_1|}j(p_1)\right]j^2(p_2)\frac{2p_{3z}^2 + p_3^2}{p_3^2}j^2(p_3) \\ & + j^2(p_1)j^2(p_2)\frac{p_{3z}^2}{p_3^2}j^2(p_3). \end{aligned} \tag{35}$$

In the nonrelativistic limit one has $j(p) = 0$ and thus $D^V(p_1, p_2, p_3) = D^T(p_1, p_2, p_3)$. The expression for the axial case can be found in [10].

A. 3Q scalar integrals

In the 3Q sector there is no quark-antiquark pair. There are then two integrals only, one for the vector case

$$\Phi^V(0, 0) \tag{36}$$

and one for the tensor one

$$\Phi^T(0, 0), \tag{37}$$

where the null argument indicates that the whole baryon momentum is carried by the three discrete-level quarks. Let us remind that in this sector, spin-flavor wave functions obtained by the projection technique are equivalent to those given by $SU(6)$ symmetry. One then naturally obtains the same results for the charges as those given by $SU(6)$ NQM, except that tensor quantities are multiplied by the factor $\Phi^T(0, 0)/\Phi^V(0, 0)$. As discussed in the Appendix, this is similar to the usual approach based on the Melosh rotation [15]. Note that the similitude exists on the 3Q level only since higher Fock components break the $SU(6)$ symmetry.

B. 5Q scalar integrals

In the 5Q sector there is one quark-antiquark pair and only six integrals are needed. These integrals can be written in the general form

$$K_J^I = \frac{M^2}{2\pi}\int\frac{d^3\mathbf{q}}{(2\pi)^3}\Phi^I\left(\frac{q_z}{\mathcal{M}}, \mathbf{q}_\perp\right)\theta(q_z)q_z G_J(q_z, \mathbf{q}_\perp), \tag{38}$$

where G_J is a quark-antiquark probability distribution and $J = \pi\pi, 33, \sigma\sigma$. These distributions are obtained by contracting two quark-antiquark wave functions $W(\mathbf{p}, \mathbf{p}')$, see Eq. (9) and regularized by means of the Pauli-Villars procedure

$$G_{\pi\pi}(q_z, \mathbf{q}_\perp) = \Pi^2(\mathbf{q})\int_0^1 dy\int\frac{d^2\mathcal{Q}_\perp}{(2\pi)^2}\left[\frac{\mathcal{Q}_\perp^2 + M^2}{(\mathcal{Q}_\perp^2 + M^2 + y(1-y)\mathbf{q}^2)^2} - (M \to M_{\rm PV})\right], \tag{39a}$$

$$G_{33}(q_z, \mathbf{q}_\perp) = \frac{q_z^2}{\mathbf{q}^2}G_{\pi\pi}(q_z, \mathbf{q}_\perp), \tag{39b}$$

$$G_{\sigma\sigma}(q_z, \mathbf{q}_\perp) = \Sigma^2(\mathbf{q})\int_0^1 dy\int\frac{d^2\mathcal{Q}_\perp}{(2\pi)^2}\left[\frac{\mathcal{Q}_\perp^2 + M^2(2y-1)^2}{(\mathcal{Q}_\perp^2 + M^2 + y(1-y)\mathbf{q}^2)^2} - (M \to M_{\rm PV})\right], \tag{39c}$$

where $q_z = z\mathcal{M} = (z_4 + z_5)\mathcal{M}$ and $\mathbf{q}_\perp = \mathbf{p}_{4\perp} + \mathbf{p}_{5\perp}$.

There are three integrals in the vector case

$$K^V_{\pi\pi}, K^V_{33}, K^V_{\sigma\sigma} \tag{40}$$

and three others in the tensor one

$$K^T_{\pi\pi}, K^T_{33}, K^T_{\sigma\sigma}. \tag{41}$$

Sea quarks and antiquarks do not contribute to the tensor charge since the tensor operator is chiral odd. In this approach it is reflected by the fact that the contraction of two quark-antiquark wave functions $W(\mathbf{p}, \mathbf{p}')$ with the tensor operator leaves only vanishing scalar overlap integrals $\int d^2\mathcal{Q}_\perp \mathcal{Q}_x$ or $\int d^2\mathcal{Q}_\perp \mathcal{Q}_y$.

Even though sea quarks and antiquarks do not contribute to the tensor charge, it is not sufficient to restrict the computation to the $3Q$ sector, where only discrete-level quarks appear. Higher Fock states change the composition of the discrete-level sector as shown by Eq. (13). So hidden flavors can access to the discrete-level and thus contribute to tensor charge of the baryon. In other words, even though only discrete-level quarks contribute, $SU(6)$ relations are broken due to relativistic effects (additional quark-antiquark pairs).

VI. RESULTS

A. Combinatoric results

In this work we have studied tensor charges in flavor $SU(3)$ symmetry. Even though this symmetry is broken in nature, this gives quite a good estimation. The interesting thing is that this symmetry relates tensor charges within each multiplet. Indeed all particles in a given representation are on the same footing and are related through pure flavor $SU(3)$ transformations. One can find the way to relate tensor charges of different members of the same multiplet in [10].

The octet, decuplet, and antidecuplet normalizations in the $3Q$ and $5Q$ sectors are given by the following linear combinations:

$$\mathcal{N}^{(3)}(B_{\mathbf{8}}) = 9\Phi^V(0,0),$$
$$\mathcal{N}^{(5)}(B_{\mathbf{8}}) = \tfrac{18}{5}(11K^V_{\pi\pi} + 23K^V_{\sigma\sigma}), \tag{42a}$$

$$\mathcal{N}^{(3)}_{3/2}(B_{\mathbf{10}}) = \mathcal{N}^{(3)}_{1/2}(B_{\mathbf{10}}) = \tfrac{18}{5}\Phi^V(0,0),$$
$$\mathcal{N}^{(5)}_{3/2}(B_{\mathbf{10}}) = \tfrac{9}{5}(15K^V_{\pi\pi} - 6K^V_{33} + 17K^V_{\sigma\sigma}),$$
$$\mathcal{N}^{(5)}_{1/2}(B_{\mathbf{10}}) = \tfrac{9}{5}(11K^V_{\pi\pi} + 6K^V_{33} + 17K^V_{\sigma\sigma}), \tag{42b}$$

$$\mathcal{N}^{(5)}(B_{\overline{\mathbf{10}}}) = \tfrac{36}{5}(K^V_{\pi\pi} + K^V_{\sigma\sigma}), \tag{42c}$$

where the subscripts $3/2$, $1/2$ refer to the value of the third component of the baryon spin J_z. These normalizations have been obtained by contracting the baryon wave functions without any charge acting on the quark lines.

Here are the $3Q$ and $5Q$ contributions to the proton tensor charges

$$T^{(3)}_u(p) = 12\Phi^T(0,0), \qquad T^{(3)}_d(p) = -3\Phi^T(0,0),$$
$$T^{(3)}_s(p) = 0, \tag{43a}$$

$$T^{(5)}_u(p) = \tfrac{18}{25}(48K^T_{\pi\pi} - 7K^T_{33} + 151K^T_{\sigma\sigma}),$$
$$T^{(5)}_d(p) = \tfrac{-12}{25}(24K^T_{\pi\pi} + 19K^T_{33} + 53K^T_{\sigma\sigma}),$$
$$T^{(5)}_s(p) = \tfrac{-12}{25}(3K^T_{\pi\pi} + 8K^T_{33} + K^T_{\sigma\sigma}). \tag{43b}$$

Here are the $3Q$ and $5Q$ contributions to Δ^{++} tensor charges

$$T^{(3)}_{u,3/2}(\Delta^{++}) = \tfrac{54}{5}\Phi^T(0,0),$$
$$T^{(3)}_{d,3/2}(\Delta^{++}) = T^{(3)}_{s,3/2}(\Delta^{++}) = 0,$$
$$T^{(3)}_{u,1/2}(\Delta^{++}) = \tfrac{18}{5}\Phi^T(0,0),$$
$$T^{(3)}_{d,1/2}(\Delta^{++}) = T^{(3)}_{s,1/2}(\Delta^{++}) = 0, \tag{44a}$$

$$T^{(5)}_{u,3/2}(\Delta^{++}) = \tfrac{9}{10}(56K^T_{\pi\pi} - 17K^T_{33} + 101K^T_{\sigma\sigma}),$$
$$T^{(5)}_{d,3/2}(\Delta^{++}) = T^{(5)}_{s,3/2}(\Delta^{++}) = \tfrac{-9}{20}(8K^T_{\pi\pi} + 13K^T_{33} - K^T_{\sigma\sigma}),$$
$$T^{(5)}_{u,1/2}(\Delta^{++}) = \tfrac{3}{10}(42K^T_{\pi\pi} + 25K^T_{33} + 101K^T_{\sigma\sigma}),$$
$$T^{(5)}_{d,1/2}(\Delta^{++}) = T^{(5)}_{s,1/2}(\Delta^{++}) = \tfrac{-3}{20}(6K^T_{\pi\pi} + 19K^T_{33} - K^T_{\sigma\sigma}). \tag{44b}$$

Here is the $5Q$ contribution to the Θ^+ tensor charges

$$T^{(5)}_u(\Theta^+) = T^{(5)}_d(\Theta^+) = \tfrac{-18}{5}(K^T_{33} - K^T_{\sigma\sigma}),$$
$$T^{(5)}_s(\Theta^+) = 0. \tag{45}$$

In the $5Q$ sector of Θ^+ pentaquark, the strange flavor appears only as an antiquark as one can see from its minimal quark content $uudd\bar{s}$. That is the reason why we have found no strange contribution. But if at least the $7Q$ sector was considered, we would have obtained a nonzero contribution due to flavor components like $|uus(d\bar{s})(d\bar{s})\rangle$, $|uds(u\bar{s})(d\bar{s})\rangle$, and $|dds(u\bar{s})(u\bar{s})\rangle$.

B. Numerical results

In the evaluation of the scalar integrals we have used the constituent quark mass $M = 345$ MeV, the Pauli-Villars mass $M_{\rm PV} = 556.8$ MeV for the regularization of (39), and the baryon mass $\mathcal{M} = 1207$ MeV as it follows for the "classical" mass in the mean field approximation [11]. Choosing $\Phi^V(0,0) = 1$ we obtain in the $3Q$ sector

$$\Phi^T(0,0) = 0.9306 \tag{46}$$

and in the $5Q$ sector

$$K^V_{\pi\pi} = 0.0365, \qquad K^V_{33} = 0.0197,$$
$$K^V_{\sigma\sigma} = 0.0140, \tag{47a}$$
$$K^T_{\pi\pi} = 0.0333, \qquad K^T_{33} = 0.0180,$$
$$K^T_{\sigma\sigma} = 0.0126. \tag{47b}$$

This has to be compared with the results in the axial case [9]

$$\Phi^A(0,0) = 0.8612 \tag{48}$$

$$K^A_{\pi\pi} = 0.0300, \qquad K^A_{33} = 0.0163, \qquad K^A_{\sigma\sigma} = 0.0112. \tag{49}$$

As expected from (A14)–(A16), in the Appendix, we have the following pattern for the integrals $|V| > |T| > |A|$.

C. Discussion

We collect in Tables I, II, and III our results concerning the tensor charges at the model scale $Q_0^2 = 0.36$ GeV^2.

Several theoretical determinations of the tensor charges can be found in the literature, e.g. using the MIT bag model [2,3], QCD sum rules [25], a chiral chromodielectric model [26], the χQSM [27,28], on the light cone by means of the Melosh rotation [29], using axial-vector mesons [30] or in a quark-diquark model [31]. There are also some lattice QCD studies [32].

Usually, for the proton only δu and δd are considered. They are found not to be small and to have a magnitude similar to Δu and Δd. We agree with this observation and propose also the tensor charges for the other light multiplets together with an estimation of the strangeness contribution. One can also check that Soffer's inequality (30) is satisfied for explicit flavors using our results for the axial charges given in a previous publication [10]. However, hidden flavors, i.e. s in proton and d, s in Δ^{++}, violate the inequality.

The first experimental extraction of transversity distributions has been achieved in [33]. The authors did not give explicit values for tensor charges. The latter have however been estimated to $\delta u = 0.46^{+0.36}_{-0.28}$ and $\delta d = -0.19^{+0.30}_{-0.23}$ in [31] at the scale $Q^2 = 0.4$ GeV^2. These values are unexpectedly small compared to model predictions. However, the global analysis has been recently further refined using new data from the HERMES, COMPASS, and BELLE collaborations [34]. The actual values are now $\delta u = 0.59^{+0.14}_{-0.13}$ and $\delta d = -0.20^{+0.05}_{-0.073}$ at the scale $Q^2 = 0.8$ GeV^2. In this new analysis, the contribution of the u quark has become significantly larger. Those values appear to be close to the quark-diquark model predictions. As argued in [28], one has to be very careful with this conclusion. This agreement is related to the fact that the quark-diquark model gives the lowest predictions of all other models and lattice QCD. The tensor charge being not conserved depends strongly on the scale Q^2. In order to compare model predictions made at low scale and experimental extraction at significantly higher scale, one has to evolve the values.

The solution of the next-to-leading-order evolution equation for the tensor charge is given to next-to-leading-order accuracy [5,28] by

$$\delta q(Q^2) = \left(\frac{\alpha_s(Q^2)}{\alpha_s(Q_0^2)}\right)^{4/27}\left[1 - \frac{337}{486\pi}(\alpha_s(Q_0^2) - \alpha_s(Q^2))\right]\delta q(Q_0^2). \tag{50}$$

Because of its perturbative nature, one cannot trust this expression if the scale is too small. In the quark-diquark model, $Q_0^2 = 0.16$ GeV^2 leading to $\alpha_s(Q_0^2) \approx 1.5$. This casts serious doubts on the applicability of the perturbative evolution equation. Models usually refer to some scale around $Q_0^2 = 0.36$ GeV^2. The applicability of the perturbative evolution can also be questioned for this initial value. Note however that since transversity distributions do not couple to the gluon distributions, the evolution of the tensor charges is flavor independent. In other words, the ratios of tensor charges are scale independent and allow a more reliable comparison with the experiment. From this viewpoint, there seems to be no significant disagreement between present experimental extraction and theoretical predictions [28].

We mentioned that some tensor charges have already been computed within the χQSM. Note however that these studies have been performed in the instant-form approach. The model is the same but approximations are different. On the one hand, while in the instant-form approach one considers the limit of a large number of colors to compute the matrix elements, we used only exact three color rotations. On the other hand, while in the instant-form approach the sea is treated as a whole, we consider only the two lowest Fock components. Moreover, it seems that all previous computations in the model just involved the flavor $SU(2)$ version, while we are using the flavor $SU(3)$ version. There is also a dependence on the only free parameter of

TABLE I. Our proton tensor charges.

p^+	δu	δd	δs	$g_T^{(3)}$	$g_T^{(8)}$	$g_T^{(0)}$
$3Q$	1.241	−0.310	0	1.551	0.537	0.931
$3Q+5Q$	1.172	−0.315	−0.011	1.487	0.507	0.846

TABLE II. Our Δ^{++} tensor charges.

$\Delta^{++}_{3/2}$	δu	δd	δs	$g_T^{(3)}$	$g_T^{(8)}$	$g_T^{(0)}$
$3Q$	2.792	0	0	2.792	1.612	2.792
$3Q+5Q$	2.624	−0.046	−0.046	2.670	1.541	2.532
$\Delta^{++}_{1/2}$	δu	δd	δs	$g_T^{(3)}$	$g_T^{(8)}$	$g_T^{(0)}$
$3Q$	0.931	0	0	0.931	0.537	0.931
$3Q+5Q$	0.863	−0.016	−0.016	0.879	0.508	0.831

TABLE III. Our Θ^+ tensor charges.

Θ^+	δu	δd	δs	$g_T^{(3)}$	$g_T^{(8)}$	$g_T^{(0)}$
$3Q+5Q$	−0.053	−0.053	0	0	−0.062	−0.107

the model, which is the constituent quark mass. We used the particular value $M = 345$ MeV, while other calculations considered constituent quark masses up to $\sim$450 MeV. For all these reasons, it is not an easy job to identify exactly the origin of the differences in predictions. Anyway, the model seems to suggest that $\delta u \sim 1$ and $\delta d \sim -0.3$ in all cases.

VII. CONCLUSION

We have used the chiral-quark soliton model (χQSM) formulated in the IMF up to $5Q$ Fock component to investigate octet, decuplet, and antidecuplet tensor charges. We have obtained $\delta u = 1.172$ and $\delta d = -0.315$ at $Q_0^2 = 0.36\ \text{GeV}^2$ for the proton, which are in the range of prediction of the other models.

We have also discussed the Melosh rotations involved in the usual light-cone approach compared with our approach. Melosh rotation introduces somewhat artificially angular momentum whose origin is purely kinematical. A general light-cone wave function should in fact contain a dynamical term like in the approach used in this paper.

Usual light-cone models consider only the $3Q$ sector and thus cannot estimate the strange tensor charge δs. Even though sea quarks and antiquarks do not contribute to tensor charges, one can obtain a nonzero δs because the $5Q$ component of the nucleon allows strange quarks to access to the discrete level. Our result is $\delta s = -0.011$ and thus a negative transverse polarization of strange quarks.

ACKNOWLEDGMENTS

The results presented were obtained during a stay at Ruhr Universität Bochum, Germany. The author is grateful to RUB TP2 for its kind hospitality and to M. Polyakov for his careful reading and comments. The author is also indebted to J. Cugnon whose absence would not have permitted the present work to be done. This work has been supported by the National Funds of Scientific Research, Belgium.

APPENDIX: MORE ABOUT MELOSH ROTATION

Melosh rotation is nothing else than the unitary transformation relating free light-cone spinors $u^i_{\text{LC},\lambda}$ to conventional free instant-form spinors u^i_σ

$$u^i_{\text{LC},+} = \frac{(m_i + z_i\mathcal{M}_0)u^i_\uparrow + p^R_i u^i_\downarrow}{\sqrt{(m_i + z_i\mathcal{M}_0)^2 + \mathbf{p}^2_{i\perp}}},$$
$$u^i_{\text{LC},-} = \frac{-p^L_i u^i_\uparrow + (m_i + z_i\mathcal{M}_0)u^i_\downarrow}{\sqrt{(m_i + z_i\mathcal{M}_0)^2 + \mathbf{p}^2_{i\perp}}}. \tag{A1}$$

This rotation mixes helicity states due to a nonzero transverse momentum $\mathbf{p}_{i\perp}$. The light-cone spinor with helicity + corresponds to projection of *total* angular momentum $J_z = 1/2$ and is thus constructed from a spin $\uparrow$ state with projection of orbital angular momentum $L_z = 0$ and a spin $\downarrow$ state with projection of orbital angular momentum $L_z = 1$ expressed by the factor p^R. The light-cone spinor with helicity $-$ corresponds to projection of *total* angular momentum $J_z = -1/2$ and is thus constructed from a spin $\uparrow$ state with projection of orbital angular momentum $L_z = -1$ expressed by the factor p^L and a spin $\downarrow$ state with projection of orbital angular momentum $L_z = 0$.

In LCCQM, relativistic effects are only due to the Melosh rotation. The light-cone wave functions are obtained by applying the Melosh rotation on the spinors involved in the $SU(6)$ NQM wave functions. Observables like charges are computed by considering the overlap of two wave functions with one quark operator inserted. Consequently, Melosh rotation has only a nontrivial effect on the active quark, say the third quark.

1. Vector charge

The vector charge can be obtained in IMF by means of the *plus* component of the vector operator

$$q_{\text{LC}} \equiv \frac{1}{2P^+}\left\langle P, \frac{1}{2}\,\middle|\, \bar{\psi}_{\text{LC}}\gamma^+\psi_{\text{LC}} \,\middle|\, P, \frac{1}{2}\right\rangle = \int_0^1 dz[q(z) - \bar{q}(z)], \tag{A2}$$

where $q(z)$ (resp. $\bar{q}(z)$) is the probability of finding in IMF a quark (resp. antiquark) with fraction z of the proton longitudinal momentum. This charge is not sensitive to the quark polarization and is therefore not affected by the Melosh rotation, as one can easily check. This means that the vector charge computed with the light-cone wave functions is the same as the vector charge one obtains in NQM

$$q_{\text{LC}} = q_{\text{NQM}}. \tag{A3}$$

2. Axial charge

The axial charge can be obtained in IMF by means of the *plus* component of the axial operator

$$\Delta q_{\text{LC}} \equiv \frac{1}{2P^+}\left\langle P, \frac{1}{2}\,\middle|\, \bar{\psi}_{\text{LC}}\gamma^+\gamma^5\psi_{\text{LC}} \,\middle|\, P, \frac{1}{2}\right\rangle = \int_0^1 dz[q_+(z) - q_-(z) + \bar{q}_+(z) - \bar{q}_-(z)], \tag{A4}$$

where $q_+(z)$ (resp. $q_-(z)$) is the probability of finding in IMF a quark with fraction z of the proton longitudinal momentum and polarization parallel (resp. antiparallel) to the proton longitudinal polarization. In this case the Melosh rotation introduces a nontrivial factor M_A in the wave-function overlap [35]

$$M_A = \frac{(m_q + z_3\mathcal{M}_0)^2 - \mathbf{p}_{3\perp}^2}{(m_q + z_3\mathcal{M}_0)^2 + \mathbf{p}_{3\perp}^2}. \quad \text{(A5)}$$

This means that the axial charge computed with the light-cone wave functions is just proportional to the axial charge one obtains in NQM

$$\Delta q_{\rm LC} = \langle M_A \rangle \Delta q_{\rm NQM}, \quad \text{(A6)}$$

where the expectation value $\langle M_A \rangle$ is defined by

$$\langle M_A \rangle = \int d^3p M_A |\Psi(p)|^2, \quad \text{(A7)}$$

with $\Psi(p)$ a simple normalized momentum wave function. The calculation of the expectation value with two different wave functions (harmonic oscillator and power-law fall-off) gave $\langle M_A \rangle = 0.75$ [36].

3. Tensor charge

The tensor charge can be obtained in IMF by means of the *plus* component of the tensor operator

$$\delta q \equiv \frac{1}{2P^+}\left\langle P, \frac{1}{2} \middle| \bar\psi_{\rm LC}\gamma^+\gamma^R\psi_{\rm LC} \middle| P, -\frac{1}{2}\right\rangle, \quad \text{(A8)}$$

where $\gamma^R = (\gamma^1 + i\gamma^2)/2$. In this case, the Melosh rotation introduces a nontrivial factor M_T in the wave-function overlap [29]

$$M_T = \frac{(m_q + z_3\mathcal{M}_0)^2}{(m_q + z_3\mathcal{M}_0)^2 + \mathbf{p}_{3\perp}^2}. \quad \text{(A9)}$$

This means that the tensor charge computed with the light-cone wave functions is just proportional to the tensor charge one obtains in NQM

$$\delta q_{\rm LC} = \langle M_T \rangle \delta q_{\rm NQM}. \quad \text{(A10)}$$

From Eqs. (A5) and (A9) one naturally expects that

$$|\delta q| > |\Delta q|. \quad \text{(A11)}$$

To sum up, in LCCQM one considers that the relativistic reduction of the axial and tensor charges compared to the NQM values is only due to the kinematical quark orbital angular momentum introduced by the Melosh rotation.

4. Nonrelativistic limit and Soffer's bound

In the nonrelativistic limit $\mathbf{p}_\perp = 0$, there is no orbital angular momentum. Consequently, factors introduced because of Melosh rotation become trivial $M_A = M_T = 1$, as it should be.

It is also interesting to notice that one has

$$1 + M_A = 2M_T, \quad \text{(A12)}$$

which saturates Soffer's inequality, see Eq. (30). Since $\langle M_A \rangle = 3/4$, one obtains $\langle M_T \rangle = 7/8$ and thus

$$\delta u = 7/6, \qquad \delta d = -7/24, \qquad \delta s = 0. \quad \text{(A13)}$$

5. Comparison with our approach

As discussed in the text, our approach also includes a dynamical contribution to the quark orbital angular momentum. A vector operator acting on a one-quark line gives

$$F^\dagger F \propto h^2(p) + 2h(p)\frac{p_z}{|\mathbf{p}|}j(p) + j^2(p), \quad \text{(A14)}$$

while an axial operator gives

$$F^\dagger(\sigma_3)F \propto h^2(p) + 2h(p)\frac{p_z}{|\mathbf{p}|}j(p) + \frac{2p_z^2 - p^2}{p^2}j^2(p), \quad \text{(A15)}$$

and a tensor operator gives

$$F^\dagger(\sigma_R)F \propto h^2(p) + 2h(p)\frac{p_z}{|\mathbf{p}|}j(p) + \frac{p_z^2}{p^2}j^2(p), \quad \text{(A16)}$$

with $\sigma_R = (\sigma_1 + i\sigma_2)/2$. In the nonrelativistic limit $j(p) = 0$, all three structures coincide and no orbital angular momentum is left, as it should be. Note also that at the $3Q$ level, the Soffer's bound is also saturated. Only higher Fock components can lead to a strict Soffer's inequality.

[1] J. P. Ralston and D. E. Soper, Nucl. Phys. **B152**, 109 (1979).
[2] R. L. Jaffe and X. D. Ji, Phys. Rev. Lett. **67**, 552 (1991).
[3] R. L. Jaffe and X. D. Ji,Nucl. Phys. **B375**, 527 (1992).
[4] J. C. Collins, Nucl. Phys. **B394**, 169 (1993).
[5] V. Barone, A. Drago, and P. G. Ratcliffe, Phys. Rep. **359**, 1 (2002).
[6] D. Diakonov and V. Y. Petrov, Pis'ma Zh. Eksp. Teor. Fiz. **43**, 57 (1986) [JETP Lett. **43**, 75 (1986)]; D. Diakonov, V. Y. Petrov, and P. V. Pobylitsa, Nucl. Phys. **B306**, 809 (1988); D. Diakonov and V. Y. Petrov, arXiv:hep-ph/0009006.
[7] V. Y. Petrov and M. V. Polyakov, arXiv:hep-ph/0307077.
[8] D. Diakonov and V. Petrov, Phys. Rev. D **72**, 074009 (2005).
[9] C. Lorce, Phys. Rev. D **74**, 054019 (2006).
[10] C. Lorce, Phys. Rev. D **78**, 034001 (2008).
[11] D. Diakonov, V. Y. Petrov, and M. Praszalowicz, Nucl. Phys. **B323**, 53 (1989).
[12] V. B. Berestetskii and M. V. Terent'ev, Sov. J. Nucl. Phys. **24**, 547 (1976); **25**, 347 (1977).
[13] S. J. Brodsky, H. C. Pauli, and S. S. Pinsky, Phys. Rep.

301, 299 (1998).
[14] P. L. Chung and F. Coester, Phys. Rev. D **44**, 229 (1991).
[15] H. J. Melosh, Phys. Rev. D **9**, 1095 (1974); Z. Dziembowski, Phys. Rev. D **37**, 768 (1988).
[16] V. A. Karmanov, Nucl. Phys. **B166**, 378 (1980).
[17] S. J. Brodsky, J. R. Hiller, D. S. Hwang, and V. A. Karmanov, Phys. Rev. D **69**, 076001 (2004).
[18] G. R. Goldstein and M. J. Moravcsik, Ann. Phys. (N.Y.) **98**, 128 (1976); **142**, 219 (1982); **195**, 213 (1989).
[19] P. A. M. Dirac, Rev. Mod. Phys. **21**, 392 (1949).
[20] N. Isgur, *The New Aspects of Subnuclear Physics*, edited by A. Zichichi (Plenum, New York, 1980); J. Rosner, *Techniques and Concepts of High Energy Physics*, edited by T. Ferbel (Plenum, New York, 1980); Z. Dziembowski and L. Mankiewicz, Phys. Rev. Lett. **55**, 1839 (1985).
[21] K. Suzuki and W. Weise, Nucl. Phys. **A634**, 141 (1998).
[22] J. Soffer, Phys. Rev. Lett. **74**, 1292 (1995).
[23] G. R. Goldstein, R. L. Jaffe, and X. D. Ji, Phys. Rev. D **52**, 5006 (1995).
[24] S. D. Drell and T. M. Yan, Phys. Rev. Lett. **24**, 181 (1970).
[25] B. L. Ioffe and A. Khodjamirian, Phys. Rev. D **51**, 3373 (1995).
[26] V. Barone, T. Calarco, and A. Drago, Phys. Lett. B **390**, 287 (1997).
[27] H. C. Kim, M. V. Polyakov, and K. Goeke, Phys. Lett. B **387**, 577 (1996); P. V. Pobylitsa and M. V. Polyakov, Phys. Lett. B **389**, 350 (1996).
[28] M. Wakamatsu, Phys. Lett. B **653**, 398 (2007); Phys. Rev. D **79**, 014033 (2009).
[29] I. Schmidt and J. Soffer, Phys. Lett. B **407**, 331 (1997).
[30] L. P. Gamberg and G. R. Goldstein, arXiv:hep-ph/0106178; Phys. Rev. Lett. **87**, 242001 (2001).
[31] I. C. Cloet, W. Bentz, and A. W. Thomas, Phys. Lett. B **659**, 214 (2008).
[32] S. Aoki, M. Doui, T. Hatsuda, and Y. Kuramashi, Phys. Rev. D **56**, 433 (1997); M. Gockeler *et al.* (QCDSF Collaboration and UKQCD Collaboration), Phys. Lett. B **627**, 113 (2005).
[33] M. Anselmino, M. Boglione, U. D'Alesio, A. Kotzinian, F. Murgia, A. Prokudin, and C. Turk, Phys. Rev. D **75**, 054032 (2007).
[34] M. Anselmino, M. Boglione, U. D'Alesio, E. Leader, S. Melis, and F. Murgia, arXiv:0809.3743.
[35] B. Q. Ma, J. Phys. G **17**, L53 (1991); B. Q. Ma and Q. R. Zhang, Z. Phys. C **58**, 479 (1993).
[36] S. J. Brodsky and F. Schlumpf, Phys. Lett. B **329**, 111 (1994).